Available online at www.sciencedirect.com
SCIENCE DIRECT®
International Journal of Mass Spectrometry 233 (2004) 299–304
International Journal of Mass Spectrometry
www.elsevier.com/locate/ijms

Afterglow studies of $H_3^+(v = 0)$ recombination using time resolved cw-diode laser cavity ring-down spectroscopy

P. Macko [a], G. Bánó [b], P. Hlavenka [c], R. Plašil [c], V. Poterya [c], A. Pysanenko [c], O. Votava [d], R. Johnsen [e], J. Glosík [c,*]

[a] *Department of Plasma Physics, Faculty of Mathematics, Physics and Informatics, Comenius University, Mlynska Dolina F2, 84248 Bratislava, Slovak Republic*
[b] *Research Institute for Solid State Physics and Optics, HAS, Konkoly-Thege út 29-33 Budapest, Hungary*
[c] *Department of Electronics and Vacuum Physics, Mathematics and Physics Faculty, Charles University Prague, V Holešoviècká ch 2, Prague 8, Czech Republic*
[d] *J. Heyrovský Institute of Physical Chemistry, Academy of Sciences of the Czech Republic, Dolejškova 3, 182 23 Prague 8, Czech Republic*
[e] *Department of Physics and Astronomy, University of Pittsburgh, Pittsburgh, PA 15260, USA*

Received 28 November 2003; accepted 28 December 2003

Abstract

The recombination of spectroscopically identified $H_3^+(v = 0)$ ions with thermal electrons has been studied in pulsed afterglow plasma by means of an infrared cavity ring-down spectrometer (CRDS). Time-resolved measurements of the $H_3^+(v = 0)$ density were carried out in helium buffer gas with small admixtures of argon and hydrogen. The gas temperature was ~330 K, and the total pressure ranged from 8 to 16 mbar. The CRDS signal on the $\nu_2 = 3 \leftarrow 0$ transition of H_3^+ ($\lambda = 1.4\,\mu$m) was monitored as a function of time during the discharge afterglow. Since the absorption cross-section is known, the decay of the $H_3^+(v = 0)$ number density and hence, the recombination coefficient can be deduced. At hydrogen number densities $[H_2] = 1 \times 10^{14}$ to 8×10^{14} cm^{-3} the measured recombination rate coefficient was found to be $\alpha = (1.6 \pm 0.6) \times 10^{-7}$ cm^3 s^{-1}.

Keywords: Recombination; H_3^+ ions; Cavity ring-down spectrometer; Infrared absorption spectroscopy; Hydrogen plasma

1. Introduction

The dissociative recombination of $H_3^+(v = 0)$ ions with electrons has been studied for a long time, both experimentally and theoretically. The interest in the process was renewed when this ion species was detected in interstellar clouds as well as in the ionospheres of outer planets (see, e.g., reviews by Dalgarno [1] and Oka [2]), and by the advent of the powerful ion-storage ring (ISR) experimental technique. Although much progress has been made in recent years, an entirely satisfactory agreement between theory, experiment, and astronomical observations remains to be achieved. The history of such studies will not be presented in detail here since it has been covered adequately before (see e.g., [3]).

Two types of experiments are used for electron-ion recombination studies. Beam experiments, in the form of "merged beams" or "ion-storage-rings" (ISR) provide nearly mono-energetic cross-section data under single-collision conditions, while observation in "pulsed" or "flowing" afterglows yield thermal rate coefficients α(T). The ISR data [4,5] agree rather well with results of the recent theoretical calculations by Kokoouline and Greene [6–8]. The 300 K rate coefficients inferred from those experiments [4,5] and from the theoretical cross sections fall in the range from 6×10^{-8} to 1×10^{-7} cm^3 s^{-1}, the variation apparently being due to differing rotational state distributions of the ions. The afterglow measurements present a more complicated picture. Depending on methods used, experimental conditions, and the authors' interpretation of their results, published rate coefficients at 300 K range from below 1×10^{-8}

* Corresponding author. Tel.: +420-2-2191-2329; fax: +420-2-688-5095.
E-mail address: Juraj.Glosik@mff.cuni.cz (J. Glosík).

1387-3806/$ – see front matter © 2004 Elsevier B.V. All rights reserved.
doi:10.1016/j.ijms.2003.12.035

to $\sim 2 \times 10^{-7}\,cm^3\,s^{-1}$. This wide range of results raises the question to what extent the physical conditions under which recombination occurs play a role, or if the H_3^+ ions under study differed in their state of internal excitation. Vibrational excitation has often been invoked as having a strong influence on the recombination rate (see. e.g., Smith and Spanel [9]). However, the only afterglow experiment in which unambiguous identification of the recombining ion was achieved is that of Amano et al. [10,11] who used an infrared absorption technique to monitor the $H_3^+(v = 0)$ decay in a discharge afterglow in hydrogen at pressures from 0.1 to 1 Torr. The inferred recombination coefficient was $1.8 \times 10^{-7}\,cm^3\,s^{-1}$ at a gas temperature of 210 K. While some aspects of his experiment have been challenged [9], Amano's experimental methods are valid and, with the possible exception of his data at very low gas temperatures [12], his results must be considered as reliable.

On the other hand, our stationary-afterglow measurements (advanced integrated stationary afterglow experiment or AISA) [3,13,14] have consistently indicated that the recombination rate of H_3^+ ions depends on the partial pressure of H_2. At hydrogen densities above $1 \times 10^{12}\,cm^{-3}$ the recombination rate coefficient α was found to saturate at $\sim 1.3 \times 10^{-7}\,cm^3\,s^{-1}$, in acceptable agreement with many other determinations. However, it was also found to decline to values below $1 \times 10^{-8}\,cm^3\,s^{-1}$ at far lower hydrogen densities, that is in a pressure range that was not investigated in earlier afterglow experiments. Similar results were obtained in the study of recombination of D_3^+ ions [3,15]. Possible reasons for this behaviour have been proposed. Capture of electrons into long-lived intermediate H_3^* states, that are stabilized in a subsequent collision with an H_2 molecule, has been suggested by Gougousi et al. [16] to explain the weaker pressure dependence that they observed at higher H_2 pressures. It should be noted that these three-body recombination mechanisms were proposed at a time when available theories [17,18] predicted that binary recombination of $H_3^+(v = 0)$ should be extremely slow. The need for invoking such three-body mechanisms has been lessened by the new theoretical results since most afterglow data, especially those obtained at early afterglow times and at high H_2 concentrations, exceed the theoretical results and ISR data by only about a factor of two. Nevertheless, the observed strong decline of $\alpha(H_3^+)$ at low H_2 concentrations below the recent theoretical value appears to be real and is still in need of a satisfactory explanation.

Our previous experimental studies [3,13–15] were carried out without identification of internal excitation of recombining ions and are thus open to some criticism. Although there is no definite proof, it is quite possible and perhaps likely that the H_3^+ recombination rate depends on the vibrational state of the ions, and it is far from obvious that different afterglow and beam measurements refer to ions in a same rotational and vibrational state or distribution of states. It is the long-term goal of our current research program to investigate recombination of H_3^+ with complete characterization of their internal states under plasma conditions. As the first step towards this goal we have built a new apparatus (the Test Tube), equipped with an infrared cw-diode-laser CRDS, that can measure the density decay of ions in a specific ro-vibrational state. The first application of this method is the subject of this paper. To our knowledge this is the first time that fast ion-density evolutions have been monitored by the cw-diode laser CRDS technique. In some respects our method is similar to the absorption technique used by Amano [11], but it provides the higher sensitivity that is needed to measure the ion concentrations in afterglow plasmas at moderate electron densities (near $10^{10}\,cm^{-3}$).

While the work that we present here is, in part, a "proof-of-concept" rather than a completed project, the results show that ground-state $H_3^+(v = 0)$ ions are indeed the dominant species in helium–argon–hydrogen afterglow plasmas at high H_2 concentrations, and that the effective recombination of $H_3^+(v = 0)$ ions is fast (at $[H_2] \sim 10^{14}$ to $10^{15}\,cm^{-3}$). This again raises questions about the interpretation of the slow recombination observed in the flowing-afterglow experiment by Adams et al. [19] and Smith and Spanel [9], which was ascribed to $H_3^+(v = 0)$ ions.

2. Experimental apparatus and methods

As was mentioned in the Introduction, the Test Tube experiment was primarily designed to test the optical system that will be integrated later into our AISA experiment. Thus, the design was kept simple. Fig. 1 shows a schematic diagram of the apparatus and the optical cavity. It consists of a discharge tube, made from 4 cm (internal diameter) Pyrex tubing, and a microwave waveguide in which the plasma is generated [20]. The plasma is generated by microwave pulses, ~0.5 ms long, with a repetition frequency of ~250 Hz. The effective optical length of the plasma column is estimated to be 5 cm. Gas fillings consisted of helium buffer gas with small admixtures of argon and hydrogen. Typical gas flows are: $\Phi_{He} = 350$ sccm, $\Phi_{Ar} = 2$ sccm, $\Phi_{H2} = 0.5$–5 sccm. The total pressure in the discharge tube was 8–16 mbar. A large flow of He was used to dilute possible impurities due to outgassing from the walls during the discharge, and to protect the surface of the super mirrors from plasma-enhanced deposition.

The ion-chemical processes subsequent to the discharge pulse are the same as those in our AISA experiment and have been described in detail earlier [3,13,14]. Briefly, ions and metastable helium atoms, created during the microwave discharge, are rapidly converted to H_3^+ by a sequence of ion–molecule reactions involving Ar^+ and ArH^+ as intermediate ions. The production scheme is well known and has been previously verified by kinetic modelling and mass spectrometric observations.

The novel aspect of this experiment is the observation of the time-dependent concentration of $H_3^+(v = 0)$ by optical absorption of the $\nu_2 = 3 \leftarrow 0$ overtone band [21]. A

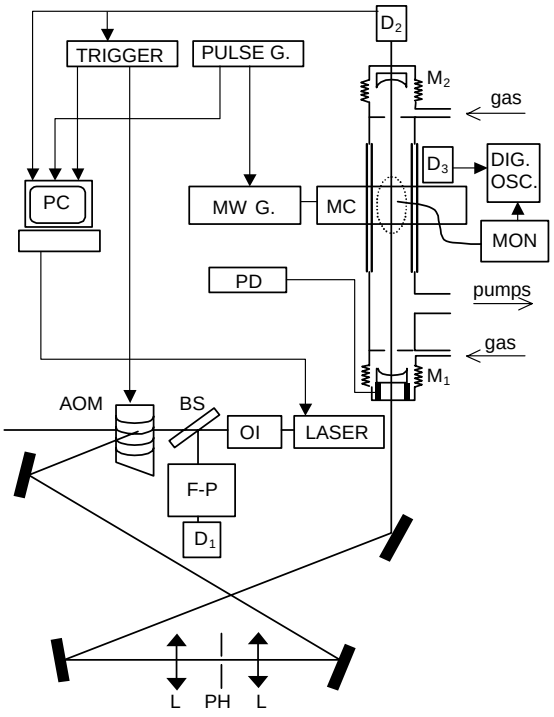

Fig. 1. The experimental set-up: OI: optical isolator, that avoids re-injection of the reflected beam into the laser diode; BS – beam-splitter; F–P: Fabry–Perot interferometer, used to monitor the frequency shift during the measurements; AOM: acousto-optical modulator; D_1: InGaAs photodiode; D_2: avalanche InGaAs photodiode; L: lenses; PH: pinhole; $M_{1,2}$: dielectric mirrors; D_3: high-frequency diode; MON: monochromator equipped with a photo-multiplier tube.

scheme of cw-cavity-ring-down spectrometer (CRDS), developed by Romanini et al. [22,23], was employed for this purpose.

The physical principles of CRDS have been described in numerous publications (see, e.g., [22,23], and references cited therein). One measures the exponential decay of the laser light intensity that is coupled into a high finesse optical cavity. The characteristic decay time depends on losses in the resonator and on absorption in the medium that is enclosed in the cavity. In our arrangement the mirrors of the optical cavity are placed at the ends of the discharge tube. A single-mode tuneable diode laser with output power of about 3 mW is used as the light source. The laser beam passes through an optical isolator that avoids re-injection of the reflected beam into the laser diode. Then the laser passes through an acousto-optic modulator (AOM). In order to suppress higher, transverse cavity modes, the laser light is also passed through a spatial filter, composed of two lenses and a pinhole of 50 μm in diameter. The optical cavity is 710 mm long. The mirrors have reflectivity of 99.995% at wavelengths near 1470 nm. In order to tune the cavity one of the mirrors is mounted on a piezoelectric transducer. This way the laser frequency can be periodically matched to one of the resonator's TEM_{00} modes. The light intensity is detected by means of an avalanche InGaAs photodiode and is digitised by a 14 bit/2 MHz PC card. When the laser wavelength matches one of the resonator's modes the light is coupled into the cavity and the photodiode signal rises rapidly. When the signal reaches the desired threshold level the laser beam is blocked by the AOM. This technique makes it possible to obtain clean and reproducible ring-down signals. In an empty resonator the characteristic time of the exponential intensity decay is ∼43 μs.

Two experimental procedures are used during the H_3^+ afterglow measurements. In the first, the laser is scanned over a certain frequency range and the CRDS signal is detected at different laser frequencies. Here, the discharge can be operated in either the continuous or the pulsed mode. The observed absorption spectra serve to identify the precise position of the H_3^+ absorption lines [20].

In the second procedure, the laser is tuned to the 6807.3 cm^{-1} transition of the $\nu_2 = 3 \leftarrow 0$ overtone band [21,24,25]. The discharge is run in the pulsed mode and the time dependence of the H_3^+ density is measured during the discharge and during the afterglow. At this stage, the periodic motion of the piezoelectric mirror holder is not yet synchronised with the discharge pulses. Hence, the whole discharge and afterglow period is randomly covered by ring-down events during numerous consecutive discharge pulses. In order to increase the frequency of the ring-down events an active tracking scheme is applied that keeps the optical cavity near the resonance position [23]. In addition, a slowly changing (active) offset is superimposed on the fast periodic motion of the piezoelectric mirror holder in order to compensate for the thermal drift of the optical cavity.

The data analysis is complicated by the fact that the H_3^+ concentration changes significantly on the time scale comparable to the cavity ring-down time, especially during the early afterglow when the $[H_3^+(v = 0)]$ concentration is large ($\sim 10^{11}$ cm^{-3}) and recombination occurs rapidly. As a consequence, the ring-down signal is close to single exponential only in the late afterglow, but not at early times. Therefore, an iterative method is used to process the data at early times. In the first iterative step, we assume that the $H_3^+(v = 0)$ density remains constant during the cavity ring-down time. In that case, the ring-down signals have a simple exponential form. We now assume that the spatial distribution of the absorbing medium does not change in time and can be described by an effective length l_{eff}. After switching the laser off, the light intensity in the resonator changes as:

$$\frac{\partial I(\nu, t)}{\partial t} = \frac{1}{\tau_{\mathrm{RD}}} I(\nu, t), \quad \text{with} \quad \frac{1}{\tau_{\mathrm{RD}}} = \frac{1}{\tau_0} + C(\nu) n(t). \quad (1)$$

Here, ν is the laser frequency, τ_0 is the ring-down time constant of the empty resonator, and $n(t) = [H_3^+(v = 0)]$ at time t. The constant C is proportional to the spectral line intensity S_{ij} (in Hitran notation [26]), absorption line profile $f(\nu)$, speed of light c, effective length l_{eff}, and is inversely proportional to the length of the resonator L: $C(\nu) = S_{\mathrm{ij}} f(\nu) c l_{\mathrm{eff}} / L$. At a given wavelength the general solution

of (1) is given by:

$$I(t) = I(t_0)\exp\left(-\frac{t-t_0}{\tau_0} - C\int_{t_0}^{t} n(t')\mathrm{d}t'\right), \quad (2)$$

where t_0 is the start time of the ring-down decay. In the first approximation, as mentioned above, we assume a constant density for each ring-down event, i.e., $n_1(t') = n_1(t_0)$. The CRDS signal is then fitted to a single exponential function and the value of $1/\tau_0 + Cn_1(t_0)$ is obtained. In the experiment the value of the empty cavity ring-down time, τ_0, can be determined from the late-afterglow data where the density $[H_3^+(v=0)]$ is negligible. In the subsequent (i-th) iteration steps $n_i(t')$ is assumed to have the form $n_i(t') = n_i(t_0) + [n_{i-1}(t') - n_{i-1}(t_0)]$. This means that we use the shape of the density variation obtained in the previous step to calculate the integral in (2) while only the $n_i(t_0)$ value (acting as an additive constant) is fitted again. This method was tested by applying it to computer-generated ring-down signals that simulate the evolution of $n(t)$. The shape of the simulated density variation was chosen to be similar to the expected experimental data, taking a constant value for the active discharge period and an abrupt fall in the afterglow. Fig. 2 shows that the procedure converges after six iteration steps and that the afterglow density decay is satisfactorily reproduced. However, artificial oscillations are still present right before the onset of the afterglow.

Because of the experimental conditions, the H_3^+ density needs to be measured most precisely in the first few hundred microseconds of the afterglow. Hence, one has to be sure that the microwave discharge has been terminated at the beginning of this time interval. Fig. 3 shows the time

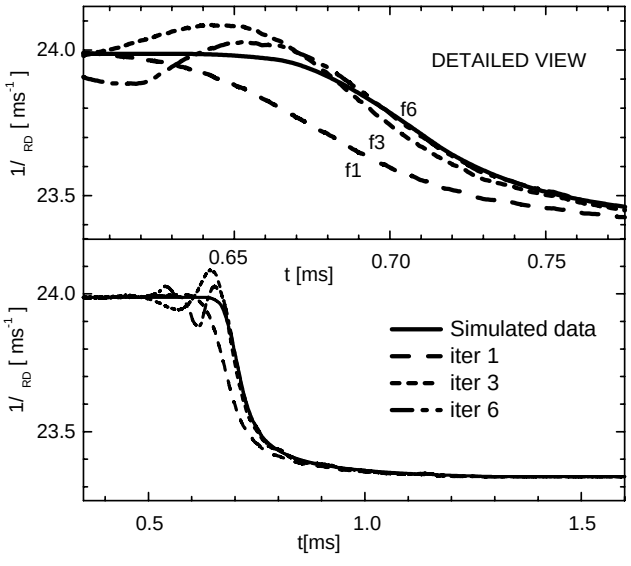

Fig. 2. Results of computer simulations testing the iterative data evaluation procedure. The time dependence of $1/\tau_{RD} = 1/\tau_0 + Cn_i$ is shown (see Eq. (1) and the subsequent explanation) as obtained from computer-generated ring-down signals by the iterative method in the i-th step. The density evolution used to create the ring-down signals is indicated by the solid curve.

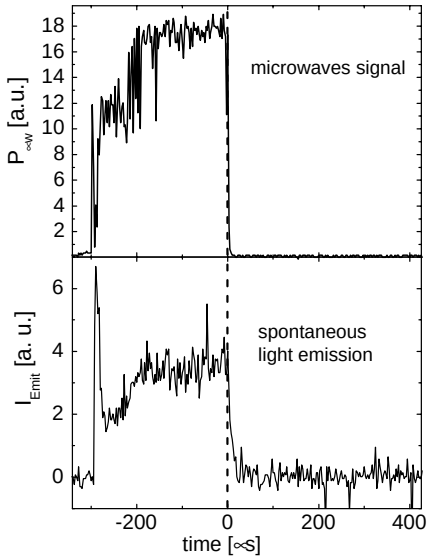

Fig. 3. The time dependence of the microwave signal and the spontaneous light intensity during the discharge and the afterglow period. The discharge is switched off at $t = 0$ s.

dependence of the microwave signal (measured in the microwave waveguide by means of the diode D_3, see Fig. 1) and the spontaneous discharge light emission. It can be seen that both signals diminish within 50 μs in the afterglow. Most probably the rate at which the light intensity signal falls is limited by the response time of the detection system.

If we assume, in agreement with the experimental result, that H_3^+ ions recombine with a rate coefficient of $\sim 10^{-7}\,\mathrm{cm^3\,s^{-1}}$, and that the overall ion density is about $3 \times 10^{11}\,\mathrm{cm^{-3}}$, we find from the balance equations that H_3^+ will be the dominant ion species at the end of the discharge. Other ion species are converted to H_3^+ within few microseconds since at $[H_2] \sim 10^{15}\,\mathrm{cm^{-3}}$ their decay time is $\tau \sim (10^{-9} \times 10^{15})^{-1}\,\mathrm{s} = 10^{-6}\,\mathrm{s}$.

3. Results and discussion

The new CRDS system was first tested on the residual H_2O vapour remaining in the discharge chamber [20]. Before the measurements the apparatus was evacuated to ~1 mbar. The laser wavelength was tuned to the region around $6805\,\mathrm{cm^{-1}}$ and was scanned through the absorption lines of the H_2O. Data taken from HITRAN 96 database [26] were used to calibrate the laser wavelength. Then the discharge tube was pumped down and the working gas mixture (helium, argon, hydrogen) was admitted to the discharge tube. Helium was purified further by a liquid nitrogen trap to suppress the residual level of H_2O. The upper panel of Fig. 4 shows a typical absorption spectrum obtained by CRDS in a continuous discharge. It covers three absorption lines in the $\nu_2 = 3 \leftarrow 0$ overtone band of $H_3^+(v=0)$. A comprehensive discussion of these lines has been given by Ventrudo et al. [21]. A detailed scan over the most intense

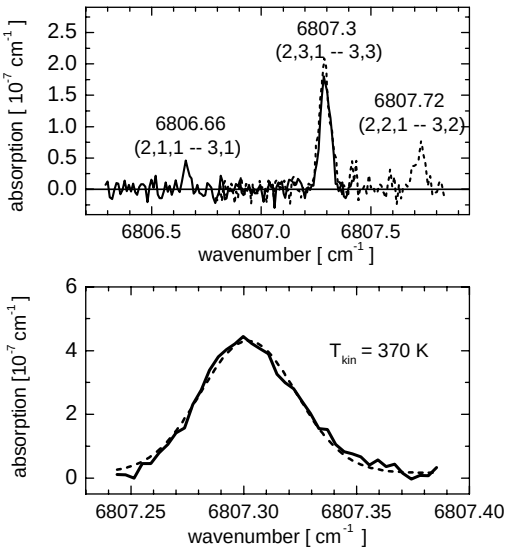

Fig. 4. Absorption spectra of $H_3^+(v=0)$ obtained in a continuous microwave discharge. Upper panel: three absorption lines in the $\nu_2 = 3 \leftarrow 0$ overtone band. Lower panel: detailed scan over the 6807.3 cm^{-1} transition. Dotted line represents calculated absorption line at 370 K.

6807.3 cm^{-1} transition (see the lower panel in Fig. 4) indicates that the Doppler linewidth (neglecting other broadening effects) corresponds to a kinetic temperature of about 370 ± 15 K in the active discharge. When the discharge is switched off, this ionic temperature decreases to the wall temperature (~330 K) within 50 μs. The accuracy of these measurements is not very high, due to rapid decrease of the absorption signal with decreasing $H_3^+(v=0)$ density. The discharge tube was warmed up during experiment. On the basis of our measurements we conclude that $H_3^+(v=0)$ are kinetically relaxed to the gas temperature during the first 50 μs, as one might expect since the ions have made several thousands of collisions with He atoms during that time.

A typical density decay of $H_3^+(v=0)$ ions in the afterglow is shown in Fig. 5. Six iteration steps (see the previous section) were used in the data reduction. The data points represent averages of approximately 2200 measured points

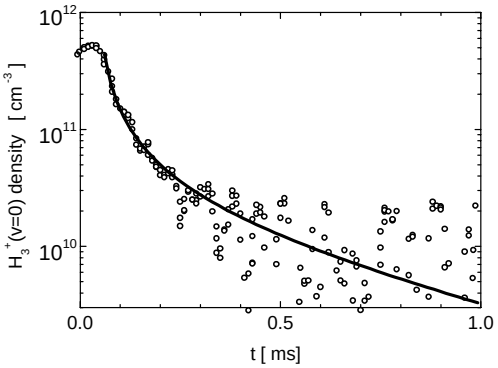

Fig. 5. Measured density decay of $H_3^+(v=0)$ ions obtained at following experimental conditions: 8 mbar of He + 0.8% Ar + 0.2% H_2 buffer gas flowing at 410 sccm.

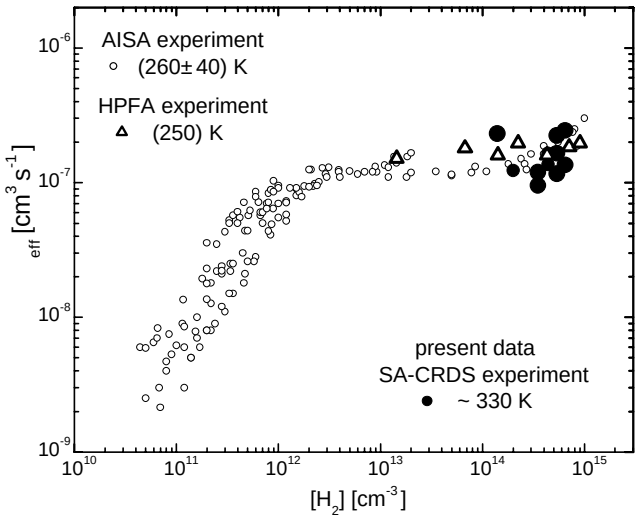

Fig. 6. Recombination coefficient of H_3^+ ions-obtained in three different afterglow experiments-plotted as a function of the hydrogen density [3,14,28]. Solid symbols represent our recent data.

per millisecond. The decay curve in Fig. 5 was fitted to an analytical formula describing recombination and diffusion losses of the ions (see e.g., [3]). Diffusion and reactions with possible impurities control the nearly exponential density decay in the late afterglow. The joint characteristic time of these diffusion–reaction losses is found to be longer than 0.5 ms. Hence, diffusion and reactions have only a minor influence on the measurement of the much faster recombination rate. The recombination rate coefficients obtained from all measured decay curves are shown in Fig. 6, together with our previous results from the AISA apparatus [3] and the high pressure flowing afterglow (HPFA) apparatus [27,28]. The data are plotted as a function of the hydrogen density. It can be seen that at a hydrogen density of $\sim 5 \times 10^{14}$ cm^{-3} the three data sets overlap very well. In the present experiment we have found the recombination rate coefficient to be $\alpha = (1.6 \pm 0.6) \times 10^{-7}$ cm^3 s^{-1}.

It should be noted that the present recombination coefficient is based on $H_3^+(v=0)$ density measurements, whereas the electron density was observed in the AISA experiments. Both methods should give the same result if $H_3^+(v=0)$ were the dominant ion species in both experiments. The good agreement between the two experiments suggests that this was the case, but it does not provide conclusive proof for the absence of other ion species, for instance H_3^+ ions in vibrational states $v > 0$. However, if vibrationally excited ions were present, they were most likely present in both experiments. The formation of $H_3^+(v=0)$ and relaxation of $H_3^+(v>0)$ ions occur in the very early afterglow, i.e., the brief period Δt between the end of the discharge and the time interval during which recombination is analysed. In the Test Tube this time is Δt (Test Tube) ≈0.05 ms; in the much larger AISA chamber this time is 300 times larger, Δt(AISA) ≈ 15 ms. Since collisions with H_2 molecules are responsible for the formation

and vibrational relaxation of H_3^+, the product $\Delta t\,[H_2]$ is the relevant quantity. It follows that one can expect similar plasma conditions in the two experiments when the hydrogen density in the Test Tube is ~300 times the hydrogen density in the AISA experiment. The above calculation tells us that $[H_2] = 1.7 \times 10^{12}\,cm^{-3}$ in the AISA experiment is equivalent to $[H_2] = 5 \times 10^{14}\,cm^{-3}$, the concentration that was used in the Test Tube. Fig. 6 shows that for these conditions both experimental techniques give essentially the same recombination rate $\alpha_{AISA}([H_2] = 1.7 \times 10^{12} cm^{-3}) \approx \alpha_{TT}([H_2] = 5 \times 10^{14}\,cm^{-3}) \approx 1 - 1.6 \times 10^{-7}\,cm^3\,s^{-1}$. This observation is consistent with the explanation that $H_3^+(v = 0)$ ions are the dominant ionic species in the afterglow period of both experiments.

4. Conclusions

Our experiments clearly demonstrate the feasibility of observing the concentration of $H_3^+(v = 0)$ ions in rapidly decaying afterglow plasma by the cavity ring-down technique. Improvements in the detection sensitivity will be needed in order to carry out such measurements at the lower ion concentrations that are present in pulsed and flowing afterglow systems. These systems allow simultaneous measurements of electron densities and are equipped with mass spectrometers, features that are essential for a complete characterization of the plasma. Also, an extension of the ring-down technique to vibrationally excited H_3^+ would be desirable.

We find that the recombination rate of $H_3^+(v = 0)$ at 330 K is $\alpha = (1.6 \pm 0.6) \times 10^{-7}\,cm^3\,s^{-1}$ at a hydrogen density of $\sim 5 \times 10^{14}\,cm^{-3}$. This value is in good agreement with results of many earlier afterglow experiments [3,11,13,14,16,29–31] and confirms the conclusions of those authors that their values refer to ground-state ions. However, the storage-ring data [4] and the recent theory [6,7] gave values that are about two times lower. The cause of this discrepancy and the fall-off of $\alpha(H_3^+)$ at low H_2 concentrations need to be explored further. In order to perform state-resolved measurements at lower hydrogen densities we plan to combine the CRDS method with the AISA apparatus [3] in the near future.

Acknowledgements

Thanks for financial support are due to GACR (205/02/0610, 202/02/0948), and MSM 1132000002. The experiments were carried out with support from EC's RTN under contract HPRN-CT-2000-0142, ETR and with support from Euroatom.

References

[1] A. Dalgarno, Mol. Opt. Phys. 32 (1994) 57.
[2] T. Oka, Phil. Trans. R. Soc. Lond. A 358 (2000) 2363.
[3] R. Plasil, J. Glosik, V. Poterya, P. Kudrna, J. Rusz, M. Tichy, A. Pysanenko, Int. J. Mass Spectrom. 218 (2002) 105.
[4] B.J. McCall, A.J. Huneycutt, R.J. Sakally, T.R. Geballe, N. Djuric, G.H. Dunn, J. Semaniak, O. Novotny, A. Al-Khalili, A. Ehlerding, F. Hellberg, S. Kalkori, A. Neau, R. Thomas, F. Österdahl, M. Larsson, Nature 422 (2003) 500.
[5] A. Wolf, in: Proceedings of the 23rd ICPEAG 2003, Progress Report, Stockholm, Sweden, July 23–29, 2003.
[6] V. Kokoouline, C.H. Greene, Phys. Rev. A 68 (2003) 012703.
[7] V. Kokoouline, C.H. Greene, Phys. Rev. Lett. 90 (2003) 133201.
[8] V. Kokoouline, C.H. Greene, B.D. Esry, Nature (Lond.) 412 (2001) 891.
[9] D. Smith, P. Spanel, Int. J. Mass Spectr. Ion Processes 129 (1993) 163.
[10] T. Amano, Astrophys. J. (1988) L 121.
[11] T. Amano, J. Chem. Phys. (1990) 6492.
[12] D.R. Bates, M.F. Guest, R.A. Kendall, Planet. Space Sci. 41 (1993) 9.
[13] J. Glosik, R. Plasil, V. Poterya, P. Kudrna, M. Tichy, Chem. Phys. Lett. 331 (2000) 209.
[14] J. Glosik, R. Plasil, V. Poterya, P. Kudrna, M. Tichy, A. Pysanenko, J. Phys. B: At. Mol. Opt. Phys. 34 (2001) L485.
[15] V. Poterya, J. Glosik, R. Plasil, M. Tichy, P. Kudrna, A. Pysanenko, Phys. Rev. Lett. 88 (2002) 044802.
[16] T. Gougousi, R. Johnsen, M.F. Golde, Int. J. Mass Spectrom. Ion Processes 149/150 (1995) 131.
[17] H.H. Michels, R.H. Hobbs, Astrophys. J. 286 (1984) L27.
[18] K.C. Kulander, M.F. Guest, J. Phys. B: Atom. Mol. Phys. 12 (1979) L501.
[19] N.G. Adams, D. Smith, E. Alge, J. Chem. Phys. 81 (1984) 1778.
[20] P. Macko, R. Plasil, P. Kudrna, P. Hlavenka, V. Poterya, A. Pysanenko, G. Bano, J. Glosik, Czechoslovak J. Phys. 52 (2002) D695.
[21] B.F. Ventrudo, D.T. Cassidy, J. Chem. Phys. 100 (1994) 6263.
[22] D. Romanini, A.A. Kachanov, F. Stoeckel, Chem. Phys. Lett. 270 (1997) 538.
[23] D. Romanini, A.A. Kachanov, N. Sadeghi, F. Stoeckel, Chem. Phys. Lett. 264 (1997) 316.
[24] T. Oka, http:/h3plus.uchicago.edu, 2003.
[25] L. Neale, S. Miller, J Tennyson, Astrophys. J. 464 (1) (1996) 516.
[26] L.S. Rothman, C.P. Rinsland, A. Goldman, S.T. Massie, D.P. Edwards, J.-M. Flaud, A. Perrin, C. Camy-Peyret, V. Dana, J.-Y. Mandin, J. Schroeder, A. McCann, R.R. Gamache, R.B. Wattson, K. Yoshino, K.V. Chance, K.W. Jucks, L.R. Brown, V. Nemtchinov, P. Varanasi, J. Quant. Spetrosc. Radiat. Transfer 60 (1998) 665 Hitran 96 database, http://cfa-www.harvard.edu/HITRAN/.
[27] A. Pysanenko, O. Novotný, P. Zakouril, R. Plasil, V. Poterya, J. Glosik, Czechoslovak J. Phys. 52 (2002) D681.
[28] J. Glosik, O. Novotný, A. Pysanenko, P. Zakouril, R. Plasil, P. Kudrna, V. Poterya, Plasma Source Sci. Technol., 12 (4) (2003) S117.
[29] A. Canosa, J.C. Gomet, B.R. Rowe, J.B.A. Mitchell, J.L. Queffelec, J. Chem. Phys. 97 (2) (1992) 1028.
[30] T. Mosbach, Besetzungsdynamik von molekularem Wasserstoff in einer magnetischen Multipol-Plasmaquelle, Cuvillier Verlag Göttingen, 2002.
[31] J.A. Macdonald, M.A. Biondi, R. Johnsen, Planet. Space Sci. 5 (1984) 651.